Theor Chem Acc (2005) 113: 205–211
DOI 10.1007/s00214-004-0625-9

REGULAR ARTICLE

Robert Ponec · Patrick Bultinck · Sofie Van Damme
Ramon Carbó-Dorca · Dean J. Tantillo

Geometric and electronic similarities between transition structures for electrocyclizations and sigmatropic hydrogen shifts

Received: 1 October 2004 / Accepted: 19 November 2004 / Published online: 7 February 2005

Abstract This paper reports new theoretical evidence that supports previous proposals concerning the similarity between transition structures for electrocyclizations and sigmatropic hydrogen shifts. This evidence was obtained using two recently proposed methodologies, namely the so-called generalized population analysis and the formalism of molecular quantum similarity indices. Analysis of multicenter bond indices shows that the transition structures for cationic [1, *n*] hydrogen shifts do indeed have three-center indices that are similar to those of other three-center carbocations. In addition, the close resemblance of the electronic structures of electrocyclic and sigmatropic transition structures that differ by only a proton is supported by the values of their quantum molecular similarity indices.

Keywords Multicenter bonding · Pericyclic reactions · Transition states · Molecular similarity

1 Introduction

Ever since the seminal work on orbital symmetry conservation by Woodward and Hoffmann [1] and the description of related concepts by Fukui [2], Zimmerman [3] and others, curiosity about the geometric and electronic properties of pericyclic transition states has grown. Countless pericyclic transition structures have been computed with many different varieties of molecular orbital theory, and trends in their properties have emerged [4]. Of particular relevance to the work described herein are the studies by Houk et al. [4] and Hoffmann and Tantillo [5] that revealed the geometric similarities (in terms of both specific bond lengths and overall shapes) between pericyclic transition structures from various reaction types, and the analyses by Jiao and Schleyer [6] of trends in the magnetic properties (nucleus-independent chemical shifts [7], magnetic susceptibilities, and their connections to aromaticity) of many different pericyclic transition structures.

The study by Hoffmann and Tantillo [5] described a set of pericyclic reactions and transition structures for different allowed and forbidden reaction paths. We now extend this analysis by quantifying the geometric and electronic similarities of various pericyclic transition structures using two recently developed computational methodologies. One is the so-called generalized population analysis [8], which is a new theoretical tool for the detection and localization of multicenter bonding in a molecule. Our second approach involves quantum molecular similarity indices [9], with which the similarity – in particular similarities in electronic structure – of various molecules can be quantified.

2 Theoretical approaches and computational methods

As described previously [5], the structures of all transition states were completely optimized and characterized by frequency analysis at the B3LYP/6-31G(d) [10] level of theory using GAUSSIAN98 [11]. Since the theoretical background of both computational methodologies used – generalized population analysis and quantum molecular similarity measurement – is thoroughly described in previous original studies [8,9], we confine ourselves here to a brief recapitulation of

R. Ponec (✉)
Institute of Chemical Process Fundamentals,
Czech Academy of Sciences,
Prague 6, Suchdol, 165 02 Czech Republic
E-mail: rponec@icpf.cas.cz

P. Bultinck · S. Van Damme
Department of Inorganic and Physical Chemistry,
Ghent University, Krijgslaan 281 (S-3),
B-9000 Gent, Belgium
E-mail: Patrick.Bultinck@UGent.be

R. Carbó-Dorca
Institute of Computational Chemistry,
University of Girona, Campus de Montilivi,
17005 Girona, Spain
E-mail: quantumqsar@hotmail.com

D.J. Tantillo
Department of Chemistry, University of California,
One Shields Avenue, Davis, CA 95616, USA
E-mail: tantillo@chem.ucdavis.edu

the basic ideas to the extent necessary for the purpose of this study.

The generalized population analysis is the generic name for the whole family of approaches [8], allowing the detection of ordinary two-center and/or nonclassical multicenter bonding interactions on the basis of the contributions, the so-called bond indices, resulting from the partitioning of the identity Eq. (1) for the appropriate values of k. The Eq. (1) holds at the Hartree–Fock (and formally also Kohn–Sham) level of the theory, and P and S denote the charge-density bond-order and overlap matrices respectively.

$$\frac{1}{2^{k-1}} Tr(PS)^k = N = \sum_A \Delta_A^{(k)} + \sum_{A<B} \Delta_{AB}^{(k)} + \sum_{A<B<C} \Delta_{ABC}^{(k)} + \cdots + \sum_{A<B<C<\cdots<K} \Delta_{ABC\cdots K}^{(k)}. \quad (1)$$

Thus, for example, the monoatomic terms resulting from the partitioning Eq. (1) for $k = 1$ are identical to the Mulliken atomic charges on the atoms. Similarly, the diatomic terms resulting from the partitioning Eq. (1) for $k = 2$ are equivalent to the so-called Wiberg or Wiberg–Mayer bond indices [12, 13], whose values are known often to coincide closely with the classical bond multiplicities of ordinary two-center two-electron (2c–2e) bonds.

Straightforward extension of the above approach for higher values of k allows one to detect and to localize the presence of nonclassical multicenter bonding. Thus, for example, the existence of the most common nonclassical bonding, namely three-center bonding, can be detected on the basis of the values of triatomic terms resulting from the partitioning Eq. (1) for $k = 3$. This approach was used previously to characterize multicenter bonding in, for example, simple atomic clusters [14], electron-deficient boranes [15], three-center two-electron carbocations [16], and five-center four-electron carbocations [17]. Here, we report the application of this technique to the detection of three-center bonding in the transition states of selected pericyclic reactions, which was suggested previously [5]. The relevant bond indices were calculated at the same B3LYP/6-31G* level of the theory using our own program, which is available upon request. This program is interfaced with the output produced by GAUSSIAN using the keywords POP = FULL and IOP(3/33 = 1); these commands provide the matrices P and S required for the calculation of the multicenter indices.

"Similarity indices" were obtained from the molecular quantum similarity theory. For full details of this theory, including the formal mathematical background, the reader is referred to Carbó-Dorca et al. [9] Briefly, the molecular quantum similarity measure (MQSM) $Z_{AB}[\Omega]$ is given by:

$$Z_{AB}[\Omega] = \iint \rho_A(\mathbf{r}_1)\, \Omega(\mathbf{r}_1, \mathbf{r}_2)\, \rho_B(\mathbf{r}_2)\, d\mathbf{r}_1 d\mathbf{r}_2, \quad (2)$$

where A and B refer to the molecules compared. $\rho_A(\mathbf{r}_1)$ and $\rho_B(\mathbf{r}_2)$ are the first-order electron densities of A and B respectively, and $\Omega(\mathbf{r}_1, \mathbf{r}_2)$ is a positive definite operator. The operator used most often is the Dirac delta function, which yields a so-called overlap-type MQSM:

$$Z_{AB} = \int \rho_A(\mathbf{r}_1)\, \rho_B(\mathbf{r}_1)\, d\mathbf{r}_1 \quad (3)$$

from which the Carbó similarity index [18] may be obtained as a generalized cosine:

$$C_{AB} = \frac{\int \rho_A(\mathbf{r}_1)\, \rho_B(\mathbf{r}_1)\, d\mathbf{r}_1}{\sqrt{\int \rho_A^2(\mathbf{r}_1)\, d\mathbf{r}_1 \int \rho_B^2(\mathbf{r}_1)\, d\mathbf{r}_1}} \quad (4)$$

The Carbó index lies in the interval [0,1], where 0 is the hypothetical limit of complete dissimilarity, and 1 denotes perfect similarity or homothecy.

Within the LCAO-MO theory, the electron densities in Eq. (4) are given by the well-known formulae [19], so the overlap MQSM becomes:

$$Z_{AB} = \sum_{\nu\mu}^{M_A} \sum_{\sigma\lambda}^{M_B} P_{\nu\mu}^A P_{\sigma\lambda}^B \times \int \phi_\nu^{A,*}(\mathbf{r}_1)\, \phi_\mu^A(\mathbf{r}_1)\, \phi_\sigma^{B,*}(\mathbf{r}_1)\, \phi_\lambda^B(\mathbf{r}_1)\, d\mathbf{r}_1. \quad (5)$$

A and B denote the molecules considered in the MQSM. M_A and M_B are the number of basis functions on A and B respectively, ϕ are the basis functions with the superscript denoting the molecule to which it belongs, and $\mathbf{P}^A$ and $\mathbf{P}^B$ are the density matrices for A and B with elements $\{P_{\nu\mu}^A\}$ and $\{P_{\sigma\lambda}^B\}$. The MQSM thus becomes a sum of integrals over four basis functions. These integrals can be calculated by repeated application of the usual expressions used for calculating overlap integrals. MQSM were calculated using programs developed in house [20] and the similarity routines of the BRABO ab initio program [21]. In the following, the density matrices were split up into core and valence contributions by limiting the summations in the calculation of the density matrix elements over the MO coefficients of the basis functions. As a result, a separate Carbó index can be reported for the similarity between the core densities and valence densities of both molecules.

MQSM like in Eq. (5) clearly depend on the molecular alignment of the molecules A and B. The molecules in this study were aligned using the QSSA algorithm developed by Bultinck et al. [22]. This program aligns the molecules in such a way that the similarity between them is maximized. All MQSM reported were calculated from the B3LYP/6-31G(d) electron densities for the optimized geometries of the different transition structures.

3 Results and discussion

The electrocyclic and sigmatropic transition structures compared in our study are shown in Fig. 1. These were reported previously in [5] and include four-electron, six-electron and eight-electron systems, systems with carbon backbones containing from four to eight carbon atoms, and neutral, anionic

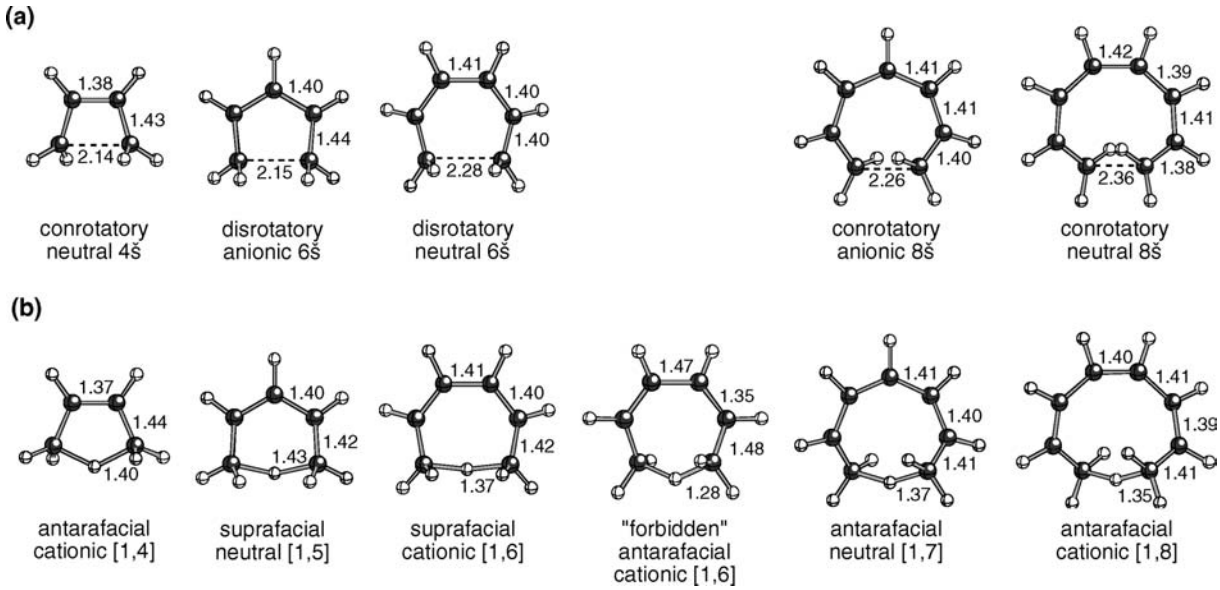

Fig. 1 Computed (B3LYP/6-31G(d)) geometries of pericyclic transition structures [5]. Selected distances are shown in Å

and cationic systems. Electrocyclic transition structures are shown in Fig. 1a, and the corresponding transition structures for the $[1, n]$ sigmatropic hydrogen shifts that would result from formal protonation of the electrocyclic transition structures [5] are shown in Fig. 1b. In addition, a transition structure for a formally forbidden [1,6] hydrogen shift (with the hydrogen migrating antarafacially with respect to the carbon backbone) [5] is also shown.

Table 1 Computed three-center bond indices for sigmatropic hydrogen shifts

Transition structure	Three-center index
Cationic [1,4]	0.216
Neutral [1,5]	0.006
Cationic [1,6]	0.130
"Forbidden" cationic [1,6]	0.312
Neutral [1,7]	0.012
Cationic [1,8]	0.098

3.1 Multicenter bond indices

Let us first discuss the similarities of the transition structures in Fig. 1 in terms of multicenter bond indices. The resemblance of the cationic $[1, n]$ sigmatropic transition structures ($n = 4, 6, 8$) in Fig. 1 to transition structures for hydride transfer from alkyl groups to carbocationic centers (as well as stable analogs of these) was discussed previously [5]. If this analogy is apt, the sigmatropic transition structures can be viewed as containing three-center two-electron (3c–2e) [C•••H•••C] fragments, with their ends linked by polyene tethers [5].

The validity of this description was tested by scrutinizing the electronic structure of the transition states using the generalized population analysis. The main emphasis was on whether the calculated three-center bond indices for the [C•••H•••C] fragments do indeed reveal the existence of significant 3c–2e bonding. The calculated values of the three-center bond indices for all of the sigmatropic transition structures from Fig. 1b (cationic and neutral) are shown in Table 1.

In order to interpret the values of these indices, one should keep in mind the analytical model of three-center bonding, whose solution yields the idealized value of the 3c–2e bond index with which the actual values can be gauged [8b]. For the bonding topology corresponding to a cationic [C•••H•••C] unit, the ideal value of the three-center index is 0.375 [8b,16].

It is clear from Table 1 that the calculated three-center indices for the $[1, n]$ sigmatropic transition states fall into two different groups, depending on their charge. The cationic $[1, n]$ sigmatropic shifts have computed indices that are lower than, but do not differ too much from, the ideal value. Thus, three-center bonding similar to that found in non-pericyclic hydride transfer transition states and related [C•••H•••C] cations [16] appears to contribute significantly to the structures of transition states for cationic $[1, n]$ sigmatropic shifts.

In addition, a systematic decrease of the calculated bond indices with the increase of the overall size of the system is observed. This implies that the importance of three-center bonding diminishes as the size of the system is increased, and the picture of bonding tends toward a more delocalized multicenter bonding array extended over the whole cyclic transition state (see below for a discussion of higher-order indices). This suggests that the tendency to form three-center bonding in [C•••H•••C] fragments apparently interferes with the tendency to equalize the carbon–carbon bond lengths in the polyenic system [4a,5]. Such an equalization is apparent not only in the values of the carbon–carbon bond

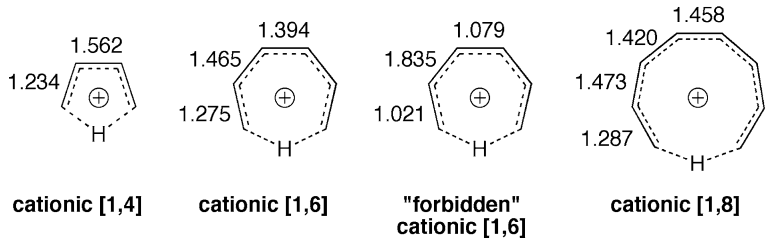

Fig. 2 Bond orders for cationic sigmatropic transition structures from Fig. 1

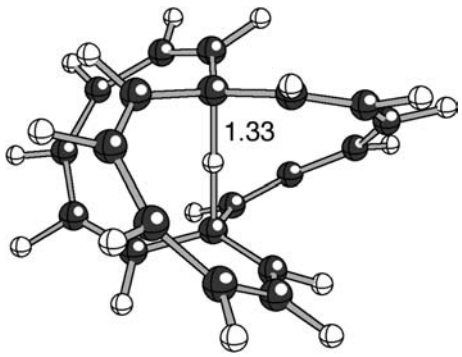

Fig. 3 "Pinwheel cation" from reference [5] (the C–H distance shown is in Å)

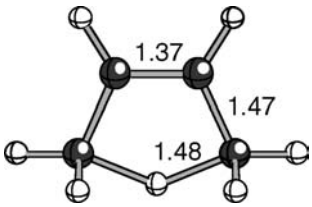

Fig. 4 Computed geometry (B3LYP/6-31G(d)) of the transition state for anionic suprafacial [1–4] hydrogen shift. Distances are shown in Å

lengths (Fig. 1), but also in the corresponding bond orders (two-center bond indices [12,13] (Fig. 2).

It is also of note that 3c–2e bonding is much more pronounced in the transition state for the thermally forbidden [1, 6] shift compared to the allowed [1,6] shift (Table 1). This was expected, given the bond lengths in these two structures (Fig. 1) [5], and is also reflected in their bond orders (Fig. 2).

Interestingly, the unusual structure shown in Fig. 3 [5] has a three-center [C•••H•••C] index of only 0.012. This structure was previously described as a hybrid between a three-center two-electron cation and three transition structures for cationic [1,8] hydrogen shifts [5]. Surprisingly, the three-center index for this structure is much lower than that of typical three-center cations as well as that for the parent cationic [1,8] shift. This suggests that there is actually very little 3c–2e bonding in this structure, and instead delocalization over the polyenyl tethers dominates.

Although 3c–2e bonding fragments exist for the cationic [1, n] transition structures, similar bonding arrays do not appear to contribute to any appreciable extent to the structures of the neutral [1,5] and [1,7] transition structures. As shown in Table 1, the calculated three-center bond indices are practically negligible for these systems. In light of what was found above, however, one can ask whether the absence of 3c–2e bonding in these systems might be compensated by a greater buildup of delocalization over the bridging hydrogen and all of the carbon atoms. The formalism of generalized population analysis has tools for directly detecting such extended multicenter bonding: the corresponding higher-order bond indices. For example, in the case of the neutral [1,5] shift, the completely delocalized transition state should extend over six centers and, consequently, it could be expected to involve six-center six-electron bonding. The existence of just this sort of bonding is indeed indicated by the calculated value of the corresponding six-center bond index, which is equal to 0.041. For comparison, the analogous six-center bond index in benzene is equal to 0.049, while that for acyclic hexatriene is 0.025.

It is also interesting that the value of the six-center bond index for the transition structure for the neutral [1,5] sigmatropic shift is also remarkably close to the value of the six-center bond index for the transition structure for thermally allowed disrotatory cyclization of hexatriene to cyclohexadiene ("neutral 6π" in Fig. 1), which is also equal to 0.041. These results reflect the "aromaticity" of these two pericyclic transition state structures [3,6,23].

Similarly, five-center six-electron bond indices for transition structures for the anionic [1,4] sigmatropic shift (Fig. 4) and the anionic 6π electrocyclization (Fig. 1) are 0.063 and 0.080, respectively. For comparison, the idealized value of the 5c–6e bond index in cyclopentadienyl anion is 0.102, while that for the acyclic pentadienyl anion is 0.069.

What about transition structures with the same number of atoms, but different numbers of electrons (and therefore different orbital topologies – suprafacial vs. antarafacial)? Consider the five-center indices for the anionic (Fig. 4) and cationic (Fig. 1) [1,4] hydrogen shifts: 0.063 and −0.059, respectively. The magnitudes of these indices are again reasonably large, indicating considerable delocalization over the four carbon atoms and the bridging hydrogen involved in each. Interestingly, the magnitudes of both indices are similar, indicating that the extent of delocalization, in terms of the orbitals involved, is essentially the same for each, even though they have different orbital topologies – one is a six-electron system involving suprafacial hydrogen migration, while the other is a four-electron system involving antarafacial hydrogen migration. The difference in the number of

Chart 1 Quantum molecular similarity Carbó indices using the total electron density, expressed as % similarity for the structures shown in Fig. 1

	Neutral 4π	Anionic 6π	Neutral 6π	Anionic 8π	Neutral 8π	Cationic [1,4]	Neutral [1,5]	Cationic [1,6]	Cationic [1,6] forbidden	Neutral [1,7]	Cationic [1,8]
Neutral 4π	100.00										
Anionic 6π	47.48	100.00									
Neutral 6π	42.24	50.36	100.00								
Anionic 8π	38.70	38.51	49.65	100.00							
Neutral 8π	36.36	38.35	43.88	53.25	100.00						
Cationic [1,4]	62.59	61.70	43.00	39.03	36.64	100.00					
Neutral [1,5]	46.83	62.66	58.30	50.80	45.93	53.14	100.00				
Cationic [1,6]	42.15	42.94	65.11	62.76	49.02	42.66	52.88	100.00			
Cationic [1,6] forbidden	42.13	49.42	69.95	44.44	40.88	43.41	58.31	52.59	100.00		
Neutral [1,7]	38.99	41.09	48.55	69.94	54.37	39.40	49.68	61.83	44.81	100.00	
Cationic [1,8]	36.45	37.98	44.14	51.94	69.58	36.79	46.69	51.42	41.16	53.82	100.00

Chart 2 Quantum molecular similarity Carbó indices using the valence electron density, expressed as % similarity, for the structures shown in Fig. 1

	Neutral 4π	Anionic 6π	Neutral 6π	Anionic 8π	Neutral 8π	Cationic [1,4]	Neutral [1,5]	Cationic [1,6]	Cationic [1,6] forbidden	Neutral [1,8]	Cationic
Neutral 4π	100.00										
Anionic 6π	80.58	100.00									
Neutral 6π	71.53	82.33	100.00								
Anionic 8π	64.26	63.38	78.27	100.00							
Neutral 8π	60.20	62.23	67.94	89.86	100.00						
Cationic [1,4]	94.02	82.83	74.56	67.74	62.52	100.00					
Neutral [1,5]	80.52	94.59	82.59	75.64	68.62	79.81	100.00				
Cationic [1,6]	69.55	80.66	96.02	78.88	71.46	73.70	75.03	100.00			
Cationic [1,6] forbidden	74.37	75.56	84.23	85.84	61.36	75.08	74.41	81.62	100.00		
Neutral [1,7]	64.91	66.84	76.67	94.50	87.35	67.30	64.95	77.79	84.71	100.00	
Cationic [1,8]	59.52	61.13	68.65	86.57	95.45	61.48	67.60	69.94	76.90	89.06	100.00

electrons involved in the five-center bonding is indicated, however, by the change in sign of the indices.

3.2 Molecular quantum similarity measures (MQSM)

We now turn to a discussion of the similarities of various pericyclic transition structures based on quantum molecular similarity indices [9]. Previous work pointed out the uniformity of carbon–carbon and carbon–hydrogen bond lengths in pericyclic transition structures, as well as the similarities in overall shape between electrocyclic and sigmatropic transition structures that differ by only a proton [4a, 5]. We now attempt to quantify the similarities of such structures using quantum molecular similarity indices. Calculated similarity indices for the set of transition structures shown in Fig. 1 are displayed in Chart 1. As described above, a distinction will be made between the total electron density and the core–core and valence–valence density similarities.

Let us now discuss the calculated similarity indices based on the total densities. First, let us concentrate on the pairs of structures for which the calculated indices imply the largest similarity and let us see how well these values correspond with the conclusions of previous studies [4a, 5]. – i.e. can the transition structures for sigmatropic [1, n] shifts be regarded as protonated versions of electrocyclic transition structures involving the same number of electrons? Let us compare the following pairs of structures: cationic [1,4] vs. neutral 4π, neutral [1,5] vs. anionic 6π, cationic [1,6] vs. neutral 6π, neutral [1,7] vs. anionic 8π, and cationic [1, 8] vs. neutral 8π. The calculated similarity indices (1) for these pairs of structures range between 63 and 70%. Consistent with expectations, similarity indices for other pairs of structures are substantially lower. For example, values for electrocyclic transition structures with the same number of electrons but different carbon backbones are 50% for the two 6π systems and 53% for the two 8π systems in Fig. 1, and the indices for sigmatropic transition structures with the same number of electrons but different carbon backbones are 53% for the neutral [1,5]/cationic [1,6] pair and 54% for the neutral [1,7]/cationic [1,8] pair.

There are also some examples which do not appear to be consistent with the expectations based on previous work [4 a, 5]. For example, consider the transition state for the formally forbidden cationic [1,6] sigmatropic shift. For this structure, an unusually high similarity (around 70%) is observed with the transition state for the thermally allowed disrotatory electrocyclic transformation of hexatriene to cyclohexadiene (neutral 6π) and also with the transition state for the neutral

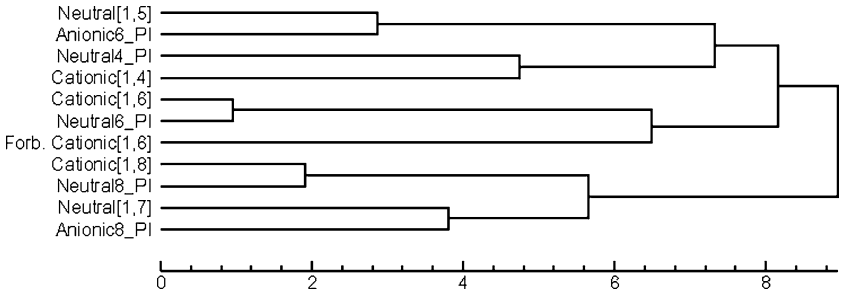

Fig. 5 Quantum molecular similarity dendrogram obtained using the valence electron density for the structures shown in Fig. 1

[1,5] sigmatropic shift (58%). The origin of these unexpected observations, however, can be traced back to the fact that total electron density similarity indices are biased by the overlap of the core regions of some atoms in the two molecules. This causes a high contribution to the MQSM. This is certainly physically sound, but chemistry is governed mainly by changes and similarities in valence electron density. In order to illustrate this, Chart 2 gives Carbó similarity indices for the valence densities of the transition structures.

It is observed that the highest similarity indices now occur only for the anticipated pairs of structures, namely cationic [1, 6] vs. neutral 6π, cationic [1, 8] vs. neutral 8π, neutral [1, 5] vs. anionic 6π, neutral [1, 7] vs. anionic 8π and cationic [1, 4] vs. neutral 4π. For each of these pairs, the Carbó index exceeds 90%. This is shown graphically, via a quantum similarity dendrogram [24], in Fig. 5.

The pairs of molecules for which high similarity was anticipated based on geometry [5] are clearly clustered very early in the dendrogram. This dendrogram also shows that, when considering valence electron density, the forbidden cationic [1, 6] transition structure is quite far from the neutral [1, 5] and allowed [1, 6] transition structures. The other pairs for which high total electron density-based similarity indices were found are now also clearly clustered at lower levels of similarity.

4 Conclusions

By examining various multicenter bond indices and quantum molecular similarity measures for the electrocyclic and sigmatropic transition structures shown in Fig. 1, we have validated two previously proposed analogies. First, the transition structures for cationic $[1, n]$ shifts have three-center indices that are similar to those of other three-center carbocations, and second, electrocyclic and sigmatropic transition structures that differ by only a proton have very high quantum molecular similarity indices. These results are in accord with previous comparisons based on geometrical considerations. Together, the analyses based on geometry [4a, 5], magnetic properties [6], multicenter bond indices, and quantum similarity measures provide a consistent picture of the bonding in pericyclic transition structures.

Acknowledgements RP acknowledges support from the grant agency of the Czech Academy of Sciences (grant No.: IAA 4072403). DJT gratefully acknowledges support from the University of California, Davis, and the National Computational Science Alliance. PB wishes to thank the Fund for Scientific Research, Flanders (Belgium) for their grants, and acknowledges the European Community, Access to Research Infrastructure action, allowing the use of the CEPBA infrastructure at the PolyTechnical University of Catalonia (Spain), and the fellowships with the Institute of Computational Chemistry at the University of Girona (Catalonia, Spain). We are also grateful to Roald Hoffmann for his insights regarding the subjects discussed herein.

References

1. (a) Woodward RB, Hoffmann R (1970) The conservation of orbital symmetry. Verlag Chemie, Weinheim; (b) Hoffmann R, Woodward RB (1968) Acc Chem Res 1:17 and references therein
2. Fukui K (1971) Acc Chem Res 4:57 and references therein
3. Zimmerman HE (1971) Acc Chem Res 4:272 and references therein. See also ref. 23
4. (a) Houk KN, Li Y, Evanseck JD (1992) Angew Chem Int Ed Engl. 31:682; (b) Wiest O, Montiel DC, Houk KN (1997) J Phys Chem A 101:8378; (c) Houk KN, Beno BR, Mendel M, Black K, Yoo HY, Wilsey S, Lee JK (1997) Theochem 398:169
5. Hoffmann R, Tantillo DJ (2003) Angew Chem Int Ed 42: 5877
6. Jiao H, Schleyer PvR (1998) J Phys Org Chem 11:655
7. (a) Schleyer PvR, Maerker C, Dransfeld A, Jiao HJ, Hommes NJRvE (1996) J Am Chem Soc 18:6317; (b) Schleyer PvR, Manoharan M, Wang ZX, Kiran B, Jiao H, Puchta R, Hommes NJRvE (2001) Org Lett 3:2465
8. (a) Ponec R, Uhlík F (1996) Croat Chem Acta 69:941; (b) Ponec R, Mayer I (1997) J Phys Chem A 101:1738; (c) Sannigrahi AB, Kar T (1990) Chem Phys Lett 173:569; (d) Sannigrahi AB, Kar T (1999) Chem Phys Lett 299:518; (e) Sannigrahi AB, Kar T (2000) Theochem 496:1; (f) Mundim KC, Giambiagi MS (1994) J Phys Chem 98:6118
9. (a) Carbó R, Calabuig B (1990) In: Johnson MA , Maggiora GM (eds), Concepts and applications of molecular similarity, Wiley Interscience, New York, pp 147–171; (b) Besalú E, Carbó R, Mestres J, Solà M (1995) Top Curr Chem 173:31; (c) Carbó-Dorca R, Besalú E (1998) J Mol Struct (Theochem) 451:11; (d) Carbó-Dorca R, Amat L, Besalú E, Lobato M (1998) In: Carbó-Dorca R, Mezey PG (eds), Advances in molecular similarity, Vol. 2, JAI, London, pp 1–42; (e) Carbó-Dorca R, Amat L, Besalú E, Gironés X, Robert D (1999) J Mol Struct (Theochem) 504; 181; (f) Carbó-Dorca R, Robert D, Amat L, Gironés X, Besalú E (2000) Lecture notes in chemistry, Vol. 73; (g) Besalu E, Girones X, Amat, Carbó-Dorca R (2002) Acc Chem Res 35:289; (h) Carbó-Dorca R, Gironés X (2003) In: Bultinck P, De Winter H, Langenaeker W, Tollenaere JP (eds), Computational medicinal chemistry for drug discovery, Dekker, New York, pp 364–386 (i) Bultinck P, Gironés X, Carbó-Dorca R In: Lipkowitz K, Cundari T (eds), Reviews in Computational Chemistry, (in press)

10. (a) Becke AD (1993) J Chem Phys 98:5648; (b) Becke AD (1993) J Chem Phys 98:1372; (c) Lee C, Yang W, Parr RG (1988). Phys Rev B 37:785; (d) Stephens PJ, Devlin FJ, Chabalowski CF, Frisch M (1994) J Phys Chem 98:11623
11. Frisch MJ, Trucks GW, Schlegel HB, Scuseria GE, Robb MA, Cheeseman JR, Zakrzewski VG, Montgomery JA, Stratmann RE, Burant JC, Dapprich S, Millam JM, Daniels AD, Kudin KN, Strain MC, Farkas O, Tomasi J, Barone V, Cossi M, Cammi R, Mennucci B, Pomelli C, Adamo C, Clifford S, Ochterski J, Petersson GA, Ayala PY, Cui Q, Morokuma K, Malick DK, Rabuck AD, Raghavachari K, Foresman JB, Cioslowski J, Ortiz JV, Stefanov BB, Liu G, Liashenko A, Piskorz P, Komaromi I, Gomperts R, Martin RL, Fox DJ, Keith T, Al-Laham MA, Peng CY, Nanayakkara A, Gonzalez C, Challacombe M, Gill PMW, Johnson BG, Chen W, Wong MW, Andres L, Head-Gordon M, Replogle ES, Pople JA (1998) GAUSSIAN98. Gaussian, Inc., Pittsburgh
12. Wiberg KB (1968) Tetrahedron 24:1083
13. (a) Mayer I (1983) Chem Phys Lett 97:270; (b) Mayer I (1986) Int J Quant Chem 29:73; (c) Mayer I (1986) Int J Quant Chem 29:477
14. Ponec R, Roithová J, Sannigrahi AB, Lain L, Torre A, Bochicchio RC (2000) Theochem 505:283
15. (a) Bochicchio RC, Ponec R, Uhlik F (1997) Inorg Chem 36:5363; (b) Ponec R, Jug K (1996) Int J Quant Chem 60:75; (c) Torre A, Lain L, Bochicchio RC, Ponec R (1999) J Comput Chem 20:1085; (d) Ponec R, Cooper DL (2004) Int J Quant Chem 97:1002
16. Ponec R, Yuzhakov G, Tantillo DJ (2004) J Org Chem 69:2992
17. Ponec R, Yuzhakov G (2003) J Org Chem 68:8284
18. Carbó R, Arnau J, Leyda L (1980) Int J Quantum Chem 17:1185
19. Szabo A, Ostlund NS (1996) Modern quantum chemistry – introduction to advanced electronic structure theory. Dover, New York
20. Van Damme S (2004) Graduation Thesis, Ghent University, Ghent Quantum Chemistry Group
21. Van Alsenoy C, Peeters A (1993) J Mol Struct (Theochem) 286:19
22. (a) Bultinck P, Kuppens T, Gironés X, Carbó-Dorca R (2003) J Chem Inf Comput Sci 43:1143; (b) Bultinck P, Carbó-Dorca R, Van Alsenoy C (2003) J Chem Inf Comput Sci 43:1208
23. Dewar MJS (1971) Angew Chem Int Ed Eng 10:761
24. Bultinck P, Carbó-Dorca R (2003) J Chem Inf Comput Sci 43:170